

Detection of human norovirus in intestinal biopsies from immunocompromised transplant patients

Umesh C. Karandikar,¹ Sue E. Crawford,¹ Nadim J. Ajami,¹
Kosuke Murakami,¹ Baijun Kou,¹ Khalil Ettayebi,¹
Genovefa A. Papanicolaou,² Ubonvan Jongwutiwes,²
Miguel-Angel Perales,^{3,4} Jinru Shia,⁵ David Mercer,⁶ Milton J. Finegold,^{7,8}
Jan Vinjé,⁹ Robert L. Atmar^{1,10} and Mary K. Estes^{1,10}

Correspondence
Mary K. Estes
mestes@bcm.edu

¹Department of Molecular Virology and Microbiology, Baylor College of Medicine, Houston, Texas 77030, USA

²Infectious Disease and Adult Bone Marrow Transplant Services, Department of Medicine, Memorial Sloan Kettering Cancer Center, New York, NY 10065, USA

³Adult Bone Marrow Transplantation Service, Memorial Sloan Kettering Cancer Center, New York, NY 10065, USA

⁴Weill Cornell Medical College, New York, NY, USA

⁵Department of Pathology, Memorial Sloan Kettering Cancer Center, New York, NY 10065, USA

⁶Department of Surgery, University for Nebraska Medical Centre, Omaha, NE 68198, USA

⁷Department of Pediatrics, Baylor College of Medicine, Houston, Texas 77030, USA

⁸Department of Pathology, Baylor College of Medicine, Houston, Texas 77030, USA

⁹Division of Viral Diseases, Centers for Disease Control and Prevention, Atlanta, Georgia, USA

¹⁰Department of Medicine, Baylor College of Medicine, Houston, Texas 77030, USA

Human noroviruses (HuNoVs) can often cause chronic infections in solid organ and haematopoietic stem cell transplant (HSCT) patients. Based on histopathological changes observed during HuNoV infections, the intestine is the presumed site of virus replication in patients; however, the cell types infected by HuNoVs remain unknown. The objective of this study was to characterize histopathological changes during HuNoV infection and to determine the cell types that may be permissive for HuNoV replication in transplant patients. We analysed biopsies from HuNoV-infected and non-infected (control) transplant patients to assess histopathological changes in conjunction with detection of HuNoV antigens to identify the infected cell types. HuNoV infection in immunocompromised patients was associated with histopathological changes such as disorganization and flattening of the intestinal epithelium. The HuNoV major capsid protein, VP1, was detected in all segments of the small intestine, in areas of biopsies that showed histopathological changes. Specifically, VP1 was detected in enterocytes, macrophages, T cells and dendritic cells. HuNoV replication was investigated by detecting the non-structural proteins, RdRp and VPg. We detected RdRp and VPg along with VP1 in duodenal and jejunal enterocytes. These results provide critical insights into histological changes due to HuNoV infection in immunocompromised patients and propose human enterocytes as a physiologically relevant cell type for HuNoV cultivation.

Received 22 June 2016
Accepted 8 July 2016

INTRODUCTION

Human noroviruses (HuNoVs) are a leading cause of acute gastroenteritis (AGE) (Koo *et al.*, 2013; Payne *et al.*, 2013; Ramani *et al.*, 2014). These non-enveloped, icosahedral viruses with a positive-sense, single-stranded RNA

genome spread via the faecal–oral route, through contaminated food, water and environmental surfaces or by direct contact (Glass *et al.*, 2009). In the USA alone, HuNoVs infect 19–21 million people and are associated with 800 deaths annually (Hall, 2012, 2013). HuNoV-mediated AGE is characterized by vomiting, diarrhoea, chills and myalgia, and is self-limiting in immunocompetent individuals (Green, 2013). However, in ‘at-risk populations’ such as the young, the elderly and the immunocompromised, HuNoV infection can cause prolonged, severe AGE (Harris *et al.*, 2008; Robilotti *et al.*, 2015; Rockx *et al.*, 2002) and be fatal in immunocompromised transplant patients (Alkhouri & Danziger-Isakov, 2011; Doshi *et al.*, 2013; Green, 2014; Roddie *et al.*, 2009; Roos-Weil *et al.*, 2011; Saif *et al.*, 2011; Schwartz *et al.*, 2011; Woodward *et al.*, 2015). Despite the awareness of disease burden and decades of research, identification of cell lines permissive for HuNoV replication has remained elusive (Duizer *et al.*, 2004; Lay *et al.*, 2010). While a recent report suggests B cells as a potential cell type permissive for replication of HuNoV *in vitro* (Jones *et al.*, 2014), HuNoV infects B cell deficient patients (Brown *et al.*, 2016) suggesting the presence of other cell types permissive for HuNoV replication in patients. One of the reasons for the lack of a robust *in vitro* culture system may be that the cell type(s) permissive for HuNoV replication in patients remain unknown. While biopsies from human volunteers experimentally infected with HuNoV show changes in the small intestinal epithelium, such as the loss of brush border enzymes and infiltration of immune cells into the lamina propria, which suggest that HuNoV replicates in the small intestine, the presence of HuNoV antigens or viral particles in patient biopsies has not been reported (Agus *et al.*, 1973; Dolin *et al.*, 1975; Schreiber *et al.*, 1973, 1974).

In this report, we address this gap in knowledge of the site and the cell type(s) permissive for HuNoV replication using intestinal biopsies from immunocompromised patients with chronic HuNoV infection. These findings will guide efforts to grow HuNoV in physiologically relevant cell types.

RESULTS

Histopathology of chronic human norovirus infection

HuNoV infections of immunocompetent volunteers result in histological changes in the small intestine such as villous blunting, infiltration of the lamina propria by immune cells, loss of nuclear polarity and flattening of the intestinal epithelium (Agus *et al.*, 1973; Dolin *et al.*, 1975; Schreiber *et al.*, 1973, 1974). To investigate if chronic HuNoV infection in immunocompromised patients results in similar changes, histological analysis was performed on 14 duodenal, 1 ileal and 4 colonic biopsies from 11 immunocompromised patients (Table 1 and Table S1, available in the online Supplementary Material). Baseline intestinal histology in the immunocompromised patients was determined by analysing biopsies from HuNoV-negative patients (Tables 1 and S1). The biopsies from HuNoV-negative patients showed normal organization of the epithelium and did not show infiltration of cells into the lamina propria (Fig. 1a, c). Duodenal biopsies from immunocompromised HuNoV-positive patients showed alterations in the gross organization of the intestinal epithelium (Fig. 1b) including loss of nuclear polarity and flattening of the villous epithelium (black bracket, Fig. 1e). However, flattening of the epithelium was not seen in the crypts (Fig. 1f). The

Table 1. Characteristics of transplant patients

Except biopsies, all the rows refer to the number of patients. NA - Not Applicable, ND - Not Determined.

Variable	Infected				Uninfected	
	HSCT	HSCT	HSCT	SBT	HSCT	SBT
Segment	Duodenum	Ileum	Colon	Jejunum	Duodenum	Jejunum
Patients	10	1	2	18	11	1
Biopsies	14*	1	4	18†	11	1‡
HuNoV strain						
GII.4	8	1	2	ND§	NA	NA
GII.2	1	0	0	ND§	NA	NA
GI.1	1	0	0	0	NA	NA
Symptoms						
Diarrhoea	9	1	2	11	0	0
Vomitus	4	0	0	4	0	0

*All the haematopoietic stem cell transplant (HSCT) biopsies were from adult patients.

†12/18 biopsies were from paediatric patients.

‡Biopsy from paediatric patient. §PCR revealed the presence of genogroup 2, but genotype specific typing was not done.

||Six patients did not exhibit diarrhoea or vomitus. Some patients were biopsied more than once; for a detailed breakdown of these biopsies, refer to Table S1.

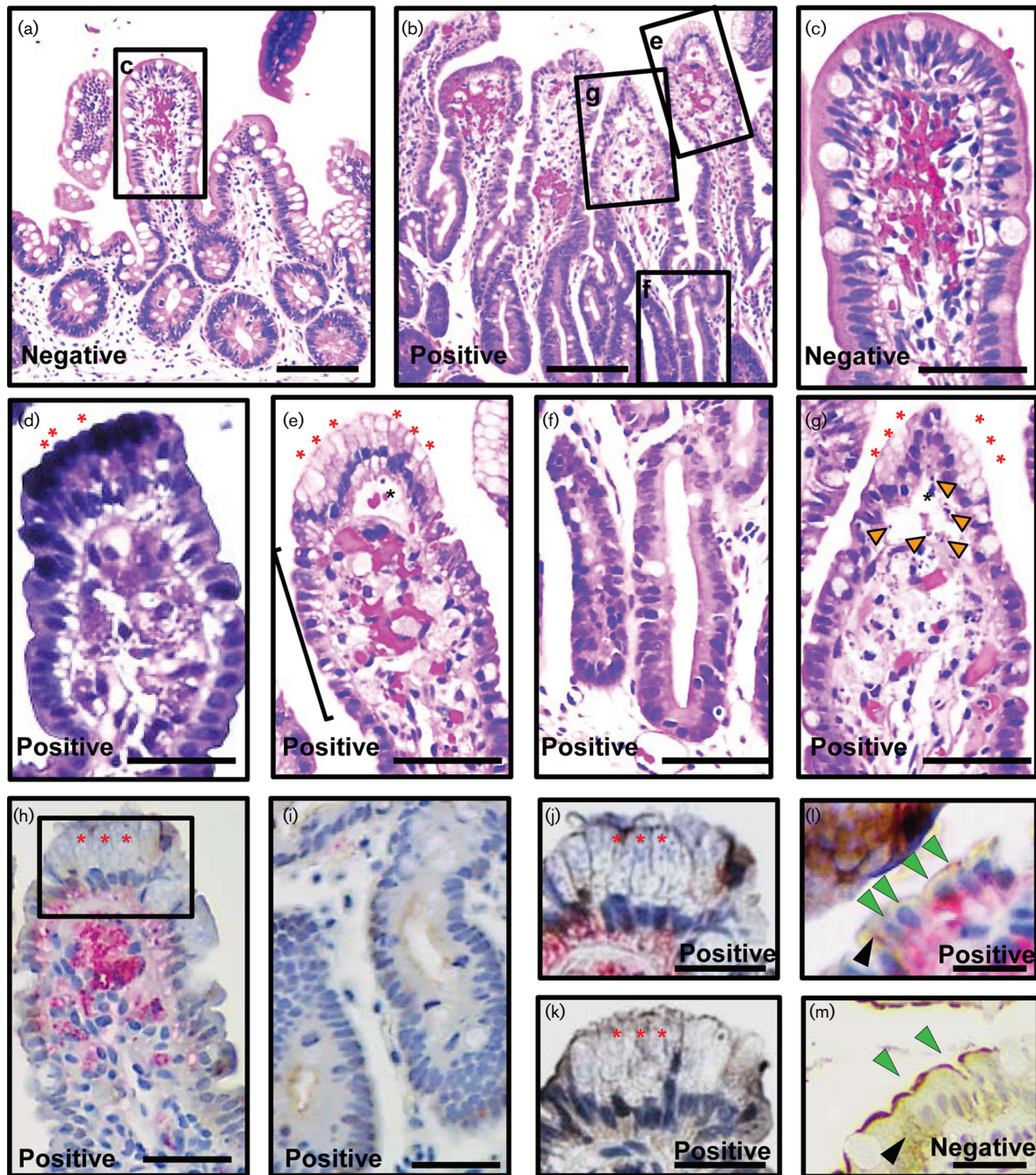


Fig. 1. HuNoV VP1 is associated with histological changes in biopsies from immunocompromised haematopoietic stem cell transplant patients. Duodenal biopsies from a HuNoV-negative (a, c and m) and HuNoV-positive (b, d–l) patients were analysed for histological changes [a–c and e–g haematoxylin and eosin (H&E) staining; d, H&E and Alcian blue–periodic acid–Schiff (Alican blue–PAS) staining to detect gastric metaplasia], and the presence of HuNoV VP1 and villin (h–m; red, VP1; brown, villin). Areas indicated by black rectangles and labelled in a and b are magnified in c and e–g, respectively; also area marked in h is magnified in j. Biopsies from the HuNoV-positive patients showed several histological changes such as loss of nuclear polarity and flattening of the epithelium (black bracket, e), gastric metaplasia (red asterisks, d, e–h, j and k), intact crypt epithelium (f and i), oedema (black asterisk, e and g), and cell debris (orange arrowheads, g). HuNoV VP1 was detected in epithelial and lamina propria cells (h, j and l) in the villi but was absent from all cells of the crypt (i). A serial section of the same biopsy stained in j showed no staining with VP1 pre-immune serum (k). VP1 was not detected in a biopsy from a HuNoV-negative patient (m). Villin expression (brown) appeared normal in the biopsy from the HuNoV-negative patient (apical expression–green arrowhead; cytosolic expression–black arrowhead, m), but was severely reduced in biopsies from the HuNoV-positive patient (h–l). VP1 was detected in enterocytes (green arrowhead, l). Bars, a and b, 100 μ m; c–k, 50 μ m; l–m 20 μ m.

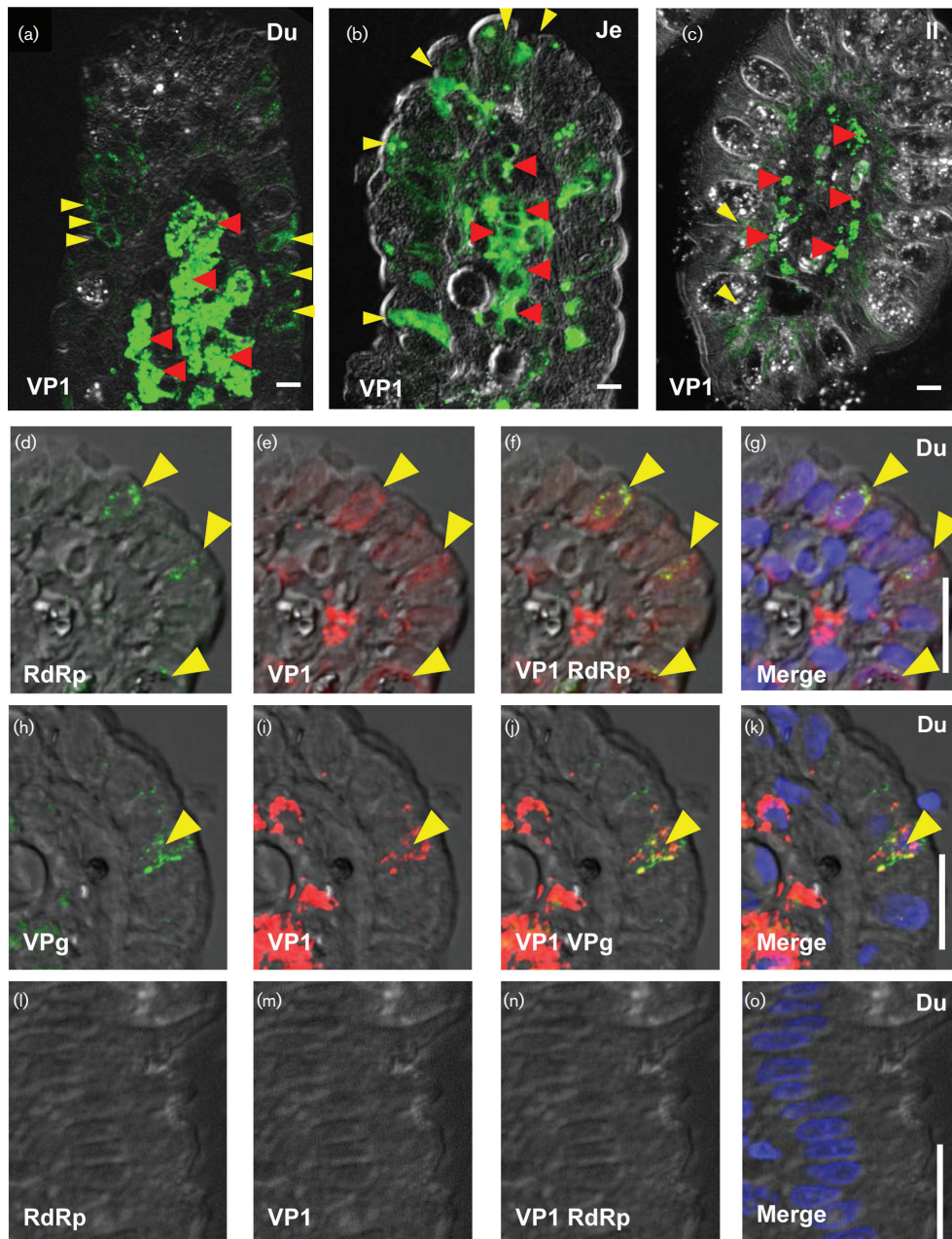


Fig. 2. Detection of HuNoV VP1, RdRp and VPg in intestinal biopsies. Immunofluorescence detection of HuNoV antigens in epithelial and lamina propria cells. HuNoV VP1 was detected in the duodenum (Du; a, e–g and i–k), jejunum (Je; b) and ileum (Il; c) in epithelial (yellow arrowheads) and lamina propria cells (red arrowheads) from HuNoV-positive patients. The non-structural proteins, RNA-dependent RNA polymerase (RdRp; d, f and g), and viral protein, genome-linked (VPg; h, j and k) were also detected in the same duodenal biopsy from a HuNoV-positive patient. Some cells showed the presence of VP1 and non-structural proteins (yellow arrowheads, d–k), while some cells showed the presence of only VP1. VP1 (m–o) and RdRp (l, n and o) were not detected in HuNoV-negative biopsies (l–o). Bars, 10 μ m.

lamina propria showed cellular infiltration (Fig. 1e, g). Oedema was seen in 9/10 patients (Table S1) as accumulation of fluid in the villi (black asterisk, Fig. 1e, g) and on rare occasions, as dilated crypts and blood vessels (data not shown). Gastric metaplasia was seen in 3/

10 patients (red asterisks, Fig. 1d, e, g and Table S1). In addition, cell debris was detected in four duodenal (orange arrowheads, Fig. 1g) and the single ileal biopsy (data not shown). Colonic biopsies from HuNoV-infected patients appeared normal. Overall, histological

analysis of the biopsies from immunocompromised patients with chronic HuNoV infection showed altered gross histology.

Human norovirus antigen is associated with histopathological changes in the small intestine

Biopsies from HuNoV-infected immunocompetent volunteers show histological changes in the small intestine (Agus *et al.*, 1973; Dolin *et al.*, 1975; Schreiber *et al.*, 1973, 1974). However, HuNoV antigens have not been detected in these biopsies. We first standardized conditions to reliably detect HuNoV VP1 in formalin-fixed, paraffin-embedded tissues (validation shown in Figs S1 and S2, available in the online Supplementary Material). We then analysed one biopsy from each of the intestinal segments from HuNoV-positive immunocompromised patients that showed histological changes.

In sections from the duodenal biopsy, VP1 (red, Fig. 1h, j, l) was detected in the epithelium with gastric metaplasia (red asterisks, Figs 1h, j and S3a) and in areas with oedema (black asterisks, Fig. S3c). No VP1 staining was detected in a matched serial section of the same duodenal biopsy stained with the VP1 pre-immune serum in the epithelium with gastric metaplasia (red asterisks, Figs 1k and S3b) and oedema (black asterisks, Fig. S3d). Duodenal biopsies from a HuNoV-negative patient did not show any staining with anti-VP1 (Fig. S3e, f) or the pre-immune sera (data not shown). VP1 was also detected in the jejunum and ileum (red, Fig. S3g–k, respectively) of HuNoV-positive patients. In both intestinal segments, VP1 was detected in areas with oedema [black asterisks, Fig. S3h (jejunum) and j (ileum), respectively]. VP1 staining was not detected in the crypts of any intestinal segment (duodenum, Fig. 1i; jejunum, Fig. S3g; ileum, Fig. S3i). Additionally, in all the sections, VP1 was localized toward the basal region of the cells in the villus epithelium. In summary, we detected VP1 in areas with histopathological changes in duodenal, jejunal and ileal biopsies from HuNoV-infected patients.

Human norovirus antigen is detected in epithelial enterocytes and cells in the lamina propria

The villous epithelium is composed of three major cell types, enterocytes, goblet cells and enteroendocrine cells. We investigated whether HuNoV antigens can be detected in each of these epithelial cell types in the HuNoV-positive biopsies. Enterocytes in the biopsies were identified using an anti-villin antibody (brown staining in a HuNoV-negative patient, Fig. 1m). The antibody detected apically-localized villin (green arrowheads, Fig. 1m) as well as villin in the cytosol of these enterocytes (black arrowhead, Fig. 1m). Overall, villin expression in HuNoV-infected patients was severely reduced in all intestinal segments (duodenum, Figs 1h–l and S3a–d; jejunum, Fig. S3g, h; ileum, Fig. 3i–k). Despite this

reduction, the villin staining was sufficient to identify VP1-positive enterocytes in these patients (villin-green and black arrowheads, VP1-red, Fig. 1l). VP1 was not detected in goblet cells or the enteroendocrine cells identified by mucin 2 and chromogranin A expression, respectively (data not shown). Based on these observations, we conclude that enterocytes are the major epithelial cell type that shows the presence of VP1. VP1 was also detected in cells of the lamina propria in these biopsies (duodenum, Figs 1h and S3a, c; jejunum, Fig. S3g and ileum, Fig. S3i, k).

We further analysed 14 duodenal (10 patients), 16 jejunal (16 patients), 1 ileal (one patient) and 4 colon biopsies (2 patients). We used E-cadherin to identify epithelial cells instead of villin due to the reduced villin expression in HuNoV-infected biopsies. We detected VP1 in the intestinal epithelium and in cells of the lamina propria of 4 duodenal biopsies (3 patients), 16 jejunal biopsies (16 patients) and in the single ileal biopsy (Table S2). We detected VP1 in 5–20 epithelial and more than 20 lamina propria cells in duodenal biopsies (Fig. 2a, Table S2). Similarly, we detected VP1 in up to 10 epithelial and 7–10 cells of the lamina propria in jejunal biopsies (Fig. 2b, Table S2). The ileal biopsy contained very few epithelial cells (3 per section) positive for VP1; in contrast, more than 20 lamina propria cells were VP1 positive (Fig. 2c, Table S2). VP1 was not detected in any of the colon biopsies (0/4) from HuNoV-infected individuals (data not shown) or in biopsies from HuNoV-negative patients (Fig. S4a, d). Together these results demonstrate that VP1 was detected mostly in enterocytes and cells in the lamina propria. Additionally, the enterocytes in HuNoV-infected cells showed severe loss of villin expression.

Human norovirus gene expression in the duodenal and jejunal epithelium

The expression of HuNoV non-structural proteins, RNA-dependent RNA polymerase (RdRp) and viral protein-genome linked (VPg), was analysed as a proxy for HuNoV replication (Lay *et al.*, 2010) in four duodenal and two jejunal biopsies that were positive for VP1. We used anti-RdRp and anti-VPg antibodies that reliably detect the respective antigens (Figs S1g–j and 2g, h). The specificity of these antibodies was validated using the respective pre-immune sera (Fig. S1o–r).

We detected RdRp (Fig. 2d, f, g) and VPg (Fig. 2h, j, k) along with VP1 (Fig. 2e–g and i–k respectively) in epithelial cells of a single duodenal biopsy (1/4). In the same biopsy, we identified multiple epithelial cells expressing RdRp and VPg (yellow arrowheads, Fig. S4g, h). We also detected RdRp along with VP1 in the epithelial cells of two jejunal biopsies (Fig. S4i–k and data not shown). In contrast, biopsies from HuNoV-negative patients did not show any staining for RdRp (Figs 2l and S4b), VPg (Fig. S4e) or VP1 (Figs 2m and S4a, d). The pre-immune sera for anti-RdRp and anti-VPg did not recognize any antigens in biopsies

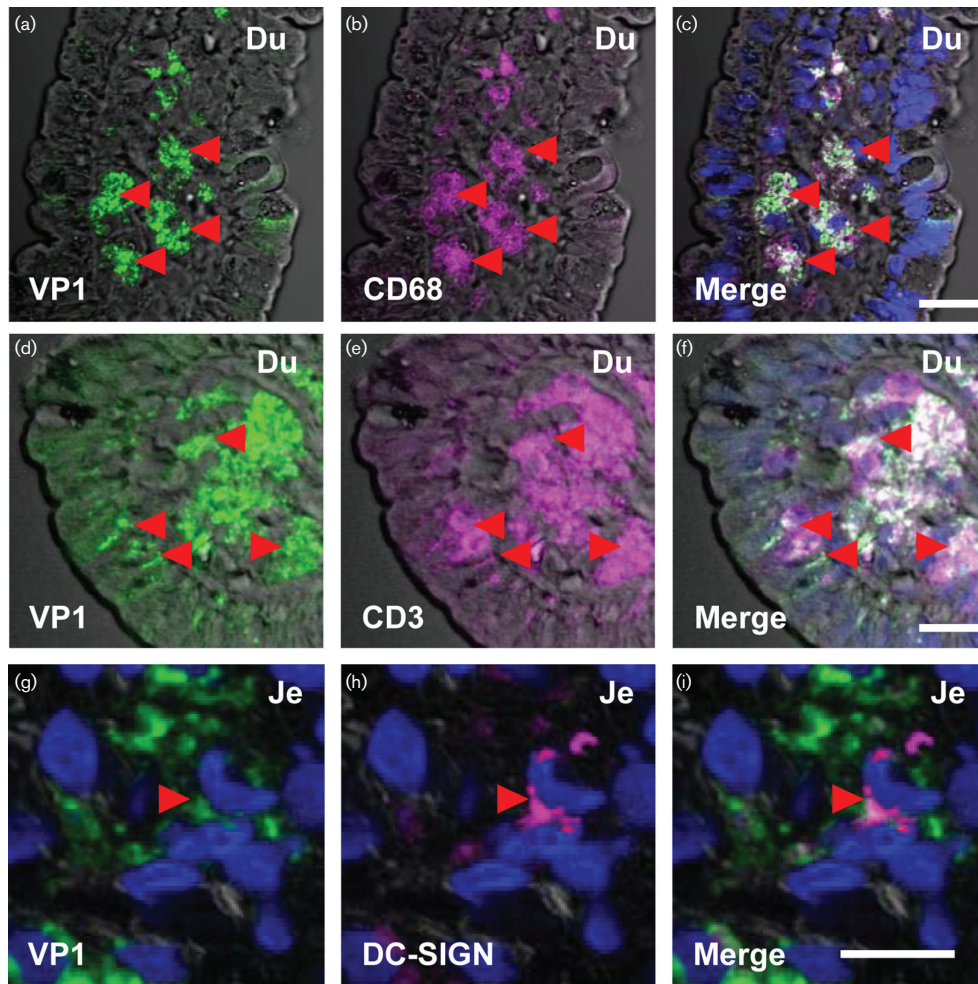


Fig. 3. Detection of HuNoV VP1 in intestinal immune cells. Immunofluorescence detection of HuNoV VP1 in the immune cells of the lamina propria. HuNoV VP1 (green) expression was analysed in duodenal (a–f) and jejunal (g–i) biopsies in the immune cells of the lamina propria. Intestinal macrophages, T cells and dendritic cells were identified based on expression of CD68 (magenta, b), CD3 (magenta, e) and DC-SIGN (magenta, h), respectively. The red arrowheads mark the position of macrophages (a–c), T cells (d–f) and dendritic cells (g–i) positive for VP1. The overlap between VP1 staining and the cell markers appear as white (c, f and i). Scale bars a–f, 50 μ m; g–i, 10 μ m.

from HuNoV-infected patients (data not shown). Thus, the presence of multiple non-structural proteins along with VP1 in the duodenal and jejunal epithelium suggests that intestinal epithelial cells support HuNoV replication.

Human norovirus VP1 is present in intestinal macrophages, dendritic cells and T cells in the lamina propria

We investigated if VP1 was present in immune cells within the lamina propria in the HuNoV-infected immunocompromised patients. We identified the immune cells using standard markers such as CD68 for macrophages, CD3 for T cells, DC-SIGN that detects a subset of dendritic cells and CD20 for B cells. We were able to detect VP1 in macrophages in all the intestinal segments

(Fig. 3a–c, Table S2). VP1 was detected in T cells in duodenal and ileal biopsies (Fig. 3d–f, Table S2). VP1 was also detected in some cells that expressed DC-SIGN in duodenal and jejunal biopsies (Fig. 3g–i, Table S2). In the ileal biopsy, VP1 staining did not overlap with cells expressing DC-SIGN (Table S2).

A recent report suggests that B cell lines can support HuNoV replication *in vitro* (Jones *et al.*, 2014). Therefore, we analysed B cells for the presence of VP1. While we were able to detect B cells in a control biopsy from a HuNoV-negative patient (1/4), B cells were not detected in four HuNoV-positive duodenal or one ileal biopsies. Two HuNoV-positive jejunal biopsies that showed CD20-positive cells did not have overlapping VP1 staining (data not shown). In summary, we detected VP1 in

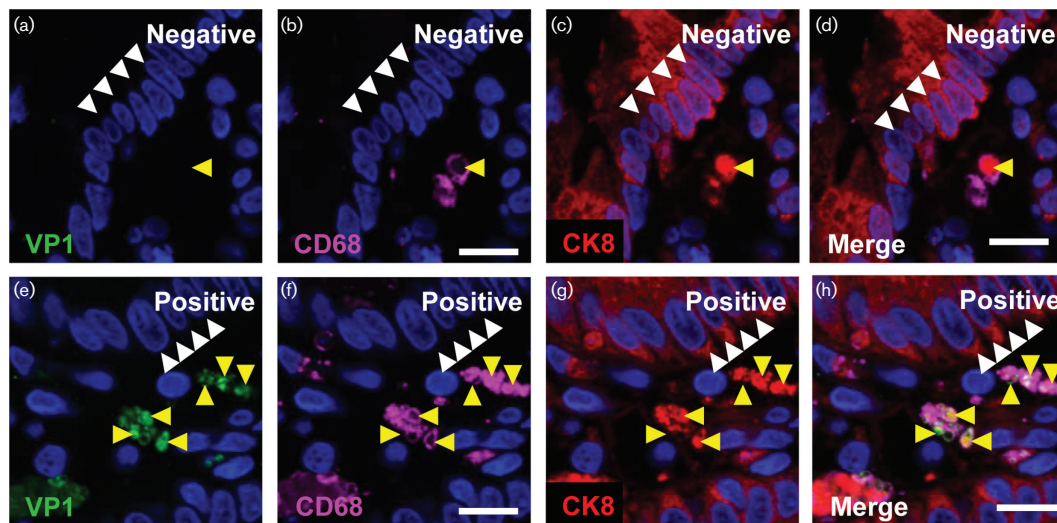


Fig. 4. Phagocytosis of HuNoV-infected epithelial cells. Immunofluorescence detection of HuNoV VP1 and epithelial marker cytokeratin 8 (CK8) in macrophages. The presence of HuNoV VP1 (green) and the epithelial marker CK8 (red) was analysed in macrophages in biopsies from a HuNoV-negative patient (a–d) and a HuNoV-positive patient (e–h). Macrophages were identified by CD68 expression (magenta). Phagocytosis of epithelial cells by the macrophages was detected by the presence of the epithelial marker CK8 (yellow arrowheads indicate position of phagocytic vesicles). In the HuNoV-negative patient, VP1 was not detected (a); however, CK8 was detected in macrophages (yellow arrowhead, d). VP1 was detected in the macrophages along with CK8 in the biopsy from the HuNoV-positive patient (yellow arrowheads, h). The white arrowheads indicate the position of the gut epithelial cells. The images shown are three optical sections from a confocal image for both the biopsies. Bars, 10 μm .

macrophages, T cells and a subset of dendritic cells in all intestinal segments.

Human norovirus antigens in the lamina propria are present in actively phagocytizing macrophages

We detected non-structural proteins VPg and RdRp along with VP1 in macrophages of the lamina propria of a duodenal biopsy from HuNoV-positive patient. The presence of HuNoV antigens in a given cell type could indicate replication, while in macrophages the presence of HuNoV antigens could also be due to phagocytosis of infected epithelial cells. To examine the latter possibility, we assessed for the epithelial marker, cytokeratin 8 (CK8) (Bimczok *et al.*, 2013), in VP1-positive macrophages in HuNoV-positive jejunal biopsies. As a control, we also analysed a biopsy from a HuNoV-negative patient. The epithelial cells showed robust CK8 expression in the biopsies from HuNoV-negative and -positive patients (white arrowheads, Fig. 4c, d, g, h, respectively). In the cells of the lamina propria from HuNoV-negative sections, CK8 was detected in macrophages in close association with the phagocytic marker CD68 (yellow arrowheads, Fig. 4b–d). VP1 was not detected in these patients (Fig. 4a). In the HuNoV-infected patient, VP1 was localized with CK8 and CD68 in the macrophages (yellow arrowheads, Fig. 4e–h). This observation was

further confirmed in duodenal biopsies from two additional patients (data not shown). The co-localization of VP1, CK8 and the CD68 suggests that macrophages can phagocytize HuNoV-infected epithelial cells in immunocompromised patients.

DISCUSSION

Intestinal biopsies from immunocompromised HuNoV-infected patients reveal several histological changes. Among the changes observed were the presence of oedema and gastric metaplasia that have not been reported in HuNoV-infected patients before. The exact contribution of HuNoV infection to the histological changes observed in the transplant patients are unclear due to the heterogeneity of the patients in terms of age, sex and presence of multiple factors associated with gastrointestinal pathology (Table S1). Despite this heterogeneity, flattening of the epithelium and severe loss of villin from the apical surface of enterocytes were observed in all HuNoV-infected patients. These observations could provide a histopathological basis for the previously reported loss of brush border enzymes located on the apical surface of enterocytes (Agus *et al.*, 1973; Schreiber *et al.*, 1973). Although VP1 was detected in all segments of the small intestine and was associated with histological changes, VP1 was detected in a subset

of the biopsies from HuNoV-positive patients. This could be due to patchy infection in the small intestine or collection of biopsies prior to detection of virus in stool (Table S1).

We detected VP1 in enterocytes in the epithelium. Importantly we also detected the presence of non-structural proteins RdRp and VPg in the epithelial cells, providing evidence that intestinal epithelial cells support HuNoV replication. Given that enterocytes are the major epithelial cells that showed the presence of VP1, it is likely that enterocytes represent a permissive cell type for HuNoV replication. This conclusion is made with the caveat that the histological studies reported here cannot prove that infectious virus is produced from the enterocytes that express non-structural and structural HuNoV proteins. B cells have been reported as a permissive cell type for HuNoV replication (Jones *et al.*, 2014); however, we did not detect VP1 in B cells. A recent study reported that HuNoV infects B cell deficient patients (Brown *et al.*, 2016). While the absence of B cells was reported to be associated with a reduction of viral titres in the patients, the overall viral titres remained high (Brown *et al.*, 2016). Together, these results suggest that B cells may not be the primary cell type for HuNoV replication *in vivo*.

We detected VP1 in immune cells such as T cells, dendritic cells and macrophages as seen generally at later times post infection in animal models. Furthermore, we detected non-structural proteins in macrophages. However, our results suggest that the presence of HuNoV antigens in macrophages could be a result of phagocytic uptake of infected epithelial cells. This observation is in agreement with previous results from our group that PBMC-derived macrophages and dendritic cells are not able to support HuNoV replication (Lay *et al.*, 2010). However, PBMC-derived macrophages and dendritic cells differ from resident immune cells found in the intestine, leaving the possibility open that HuNoV could replicate in a subset of macrophages and dendritic cells. Due to the limited number of sections from patient biopsies available for analysis, the significance of detecting VP1 in dendritic and T cells remains unclear. Thus, the question of whether HuNoV can replicate in specific subsets of intestinal immune cells needs to be investigated further.

Numerous unsuccessful attempts to cultivate HuNoVs in transformed intestinal cell lines suggest that *ex vivo*-cultured cancer cells do not support viral replication (Duiser *et al.*, 2004; Papafragkou *et al.*, 2014; Straub *et al.*, 2007; Takanashi *et al.*, 2014). We demonstrate that HuNoV can infect all segments of the small intestine and identify intestinal epithelial cells as a cell type permissive for HuNoV replication in patients. Therefore, a primary culture system derived from intestinal stem cells may be able to support HuNoV replication, which has been demonstrated recently (Ettayebi *et al.*, 2016).

METHODS

Patient description

Intestinal biopsies were obtained from patients with gastroenteritis following haematopoietic stem cell transplant (HSCT) at Memorial Sloan Kettering Center, New York, NY, USA and from small bowel transplant (SBT) patients at the University of Nebraska Medical Center, Omaha, NE, USA. PCRs were conducted as described by Vega *et al.* (2011). Sequencing of PCR products identified the genotype and strains of HuNoV in the stool samples. The study was approved by the institutional review boards of the participating institutions.

HSCT recipients with norovirus infection diagnosed between 1 January 2010 and 30 May 2012 who underwent endoscopy within 4 months of a positive norovirus test and had tissue available for examination were included in the study. In addition, stem cell recipients who underwent endoscopy for evaluation of symptoms during the same period and had a negative norovirus test within 4 months of the endoscopy served as controls. The baseline characteristics of the norovirus cases and controls are listed in the Table S1. In case of bowel transplant patients, HuNoV-positive biopsies were either from paediatric patients (12/18) or adults (6/18). The HuNoV negative biopsy was from a paediatric patient.

Haematoxylin and eosin and immunofluorescence staining of intestinal biopsies sections

The biopsies were fixed in 10% neutral buffered formalin and embedded in paraffin. The paraffin blocks containing biopsies from HuNoV-positive and -negative patients were cut in 3 µm sections. These sections were used to conduct routine haematoxylin and eosin (H&E) staining, immunohistochemistry [(IHC); as described in (Crawford *et al.*, 2006)] and immunofluorescence (IF) staining (described below). The HuNoV infection and the cell types in these paraffin sections were identified using antibodies mentioned below. The sections from HuNoV-positive and -negative patients were stained using corresponding pre-immune serum for the HuNoV antibodies and control mAb on the serial sections.

The biopsy sections were deparaffinized in xylene, followed by washes in an alcohol series (100%>100%>90%>70%). The sections were then rehydrated in water and subjected to heat-induced antigen retrieval in 10 mM citrate buffer pH 6 (Shi *et al.*, 1993). The sections were next washed in water for 5 min and blocked using blocking buffer [PBS containing a mixture of BSA and inactivated normal donkey serum (2.5% each)] for 30 min at room temperature. The sections were incubated in primary antibodies overnight at 4 °C in a humidified chamber. The following day, sections were washed three times in PBS+0.05% Tween for 10 min each. To visualize the antigens, the sections were incubated with secondary antibodies conjugated with Alexa Fluor for 2 h at room temperature, stained with DAPI (300 nM) and mounted in ProLong gold antifade (Life Technologies, Carlsbad, CA). For long-term storage, the slides were stored at -20 °C.

HuNoV antibodies. The HuNoV capsid protein VP1 was detected using a guinea pig polyclonal antiserum raised against GII.4 Sydney virus-like particles (VLPs) (anti-VP1, 1:100) and a previously described mouse monoclonal antibody, NS14 [1:100, (Kitamoto *et al.*, 2002)]. The non-structural proteins, RdRp (1:100) and the viral protein, genome-linked (VPg, 1:100), were detected using antibodies raised in rabbits against GII.3 HuNoV purified recombinant proteins (Katayama *et al.*, 2014). For validation of the antibodies to detect HuNoV antigens see supplementary figures.

Cellular antibodies. The cell types were identified using commercially available antibodies; anti-human E-cadherin (1:500, BD Biosciences,

San Jose, CA) for epithelial cells, anti-human CD68 (1:100, Sigma-Aldrich, St. Louis, MO) for macrophages, anti-human CD3 (Ready to Use, Leica, Buffalo Grove, IL) for T cells, anti-human CD20 (1:200, Leica, Buffalo Grove, IL) for B cells and anti-human DC-SIGN (10 µg ml⁻¹, Dendritics, Lyon, France) for dendritic cells. Cytokeratin was detected using anti-Cam5.2 Alexa 647 conjugate (BD Biosciences, San Jose, CA). A control monoclonal antibody [mAb 9E3-IgG1 raised against the rotavirus capsid protein VP4 (Burns *et al.*, 1988)] was used to confirm the specificity of staining with the NS14 (IgG1) monoclonal antibody.

Secondary antibodies for immunofluorescence. The secondary antibodies used for indirect IF were raised in donkey or goat and were conjugated with Alexa 488, Alexa 555 and Alexa 647 (1:1000, Life Technologies, Carlsbad, CA).

Secondary antibodies for immunohistochemistry. Dual colour IHC was carried out with goat anti-guinea pig-alkaline phosphatase and goat anti-mouse-HRP (Vector Laboratories, Burlingame, CA, as per manufacturer's recommendation).

Confocal microscopy. IF images were acquired using a Nikon A1-R confocal laser scanning microscope as previously described (Criglar *et al.*, 2014). The images for the biopsy sections along with their corresponding controls were captured using identical parameters to allow comparison between the antibodies and the pre-immune sera. The confocal stacks were captured using Nikon NIS capture software. The confocal stacks were projected in ImageJ (Fiji) and the final images were prepared in Adobe Photoshop.

Light Microscopy. Images for H&E and IHC were captured on a Nikon Eclipse Ci-L light microscope with a Nikon DS-Fi2 camera.

Validation of antibodies for detection of human norovirus antigens in formalin-fixed, paraffin-embedded samples by immunofluorescence

The ability of antibodies to detect HuNoV antigens was validated using formalin-fixed, paraffin-embedded HEK 293FT (HEK) cells expressing HuNoV proteins.

Expression of human norovirus proteins in HEK cells. HEK cells were transfected with pCG-HoV-VP1 to express the major capsid protein VP1 from GII.4 Houston virus (HoV) (Vongpunswad *et al.*, 2013). The GII.4 HuNoV non-structural proteins were produced in HEK cells by transfecting the pHuNoV_{Saga1F} construct that expresses the full length genome of GII.4 Saga1 (Katayama *et al.*, 2014). HEK cells transfected with pHuNoV_{U201F} that expressed the full-length genome of a GII.3 HuNoV served as the positive control for IF staining with anti-RdRp and anti-VPg (Katayama *et al.*, 2014). HEK cells transfected with the empty vector and mock-transfected cells served as negative controls (Katayama *et al.*, 2014). All the constructs were transfected into HEK cells by using Lipofectamine 3000 (Invitrogen Carlsbad, CA) following the manufacturer's instructions.

Fixation and sample preparation. The transfected HEK cells were harvested at 48 h post transfection. The cell pellets were fixed overnight in buffered 10 % formalin at 4 °C and embedded in paraffin. The paraffin blocks were cut into 3 µm paraffin sections for validation studies.

Detection of human norovirus antigens using indirect immunofluorescence. The HuNoV antigens in the sections of HEK cell pellets were detected by indirect IF as described above.

NOTE ADDED IN PROOF

While this article was in press, the ability of enterocytes to support HuNoV replication was reported (Ettayebi *et al.*, 2016).

ACKNOWLEDGEMENTS

Authors would like to thank Sasirekha Ramani (Dept MVM, BCM) for her critical reading of the manuscript and Pamela Parsons (Cellular and Molecular Morphology Core) for her technical assistance. This research was funded in part by Public Health Service grants NIH P01 AI057788, NIH P30 DK56338 and P30 CA125123; by Agriculture and Food Research Initiative competitive grant 2011-68003-30395 from the USDA National Institute of Food and Agriculture and by the John S. Dunn Research Foundation. Sectioning and Imaging in the Cellular Molecular Morphology Core was supported by P30 DK-56338, which funds the Texas Medical Center Digestive Diseases Center. The findings and conclusions in this article are those of the authors and do not necessarily represent the official position of the Centers for Disease Control and Prevention.

REFERENCES

- Agus, S. G., Dolin, R., Wyatt, R. G., Tousimis, A. J. & Northrup, R. S. (1973). Acute infectious nonbacterial gastroenteritis: intestinal histopathology. Histologic and enzymatic alterations during illness produced by the Norwalk agent in man. *Ann Intern Med* **79**, 18–25.
- Alkhouri, N. & Danziger-Isakov, L. (2011). Norovirus and severe chronic gastroenteritis in pediatric stem cell transplantation: the plot thickens. *Pediatr Transplant* **15**, 671–672.
- Bimczok, D., Smythies, L. E., Waites, K. B., Grams, J. M., Stahl, R. D., Mannon, P. J., Peter, S., Wilcox, C. M., Harris, P. R. & other authors (2013). *Helicobacter pylori* infection inhibits phagocyte clearance of apoptotic gastric epithelial cells. *J Immunol* **190**, 6626–6634.
- Brown, J. R., Gilmour, K. & Breuer, J. (2016). Norovirus infections occur in B cell deficient patients. *Clin Infect Dis* **62**, 1136–1138.
- Burns, J. W., Greenberg, H. B., Shaw, R. D. & Estes, M. K. (1988). Functional and topographical analyses of epitopes on the hemagglutinin (VP4) of the simian rotavirus SA11. *J Virol* **62**, 2164–2172.
- Crawford, S. E., Patel, D. G., Cheng, E., Berkova, Z., Hyser, J. M., Ciarlet, M., Finegold, M. J., Conner, M. E. & Estes, M. K. (2006). Rotavirus viremia and extraintestinal viral infection in the neonatal rat model. *J Virol* **80**, 4820–4832.
- Criglar, J. M., Hu, L., Crawford, S. E., Hyser, J. M., Broughman, J. R., Prasad, B. V. & Estes, M. K. (2014). A novel form of rotavirus NSP2 and phosphorylation-dependent NSP2-NSP5 interactions are associated with viroplasm assembly. *J Virol* **88**, 786–798.
- Dolin, R., Levy, A. G., Wyatt, R. G., Thornhill, T. S. & Gardner, J. D. (1975). Viral gastroenteritis induced by the Hawaii agent. Jejunal histopathology and serologic response. *Am J Med* **59**, 761–768.
- Doshi, M., Woodwell, S., Kelleher, K., Mangan, K. & Axelrod, P. (2013). An outbreak of norovirus infection in a bone marrow transplant unit. *Am J Infect Control* **41**, 820–823.
- Duizer, E., Schwab, K. J., Neill, F. H., Atmar, R. L., Koopmans, M. P. & Estes, M. K. (2004). Laboratory efforts to cultivate noroviruses. *J Gen Virol* **85**, 79–87.
- Ettayebi, K., Crawford, S. E., Murakami, K., Broughman, J. R., Karandikar, U., Tenge, V. R., Neill, F. H., Blutt, S. E., Zeng, X. L. & other authors (2016). Replication of human noroviruses in stem cell-derived human enteroids. *Science*. [Epub ahead of print] PMID:27562956 DOI:10.1126/science.aaf5211.

- Glass, R. I., Parashar, U. D. & Estes, M. K. (2009). Norovirus gastroenteritis. *N Engl J Med* **361**, 1776–1785.
- Green, K. Y. (2013). Caliciviridae: the noroviruses. In *Fields Virology*, 6th edn, pp. 582–608. Edited by H. P. Knipe & P. M. Howley. Philadelphia: Wolters Kluwer.
- Green, K. Y. (2014). Norovirus infection in immunocompromised hosts. *Clin Microbiol Infect* **20**, 717–723.
- Hall, A. J. (2012). Noroviruses: the perfect human pathogens? *J Infect Dis* **205**, 1622–1624.
- Hall, A. J., Lopman, B. A., Payne, D. C., Patel, M. M., Gastañaduy, P. A., Vinjé, J. & Parashar, U. D. (2013). Norovirus disease in the United States. *Emerg Infect Dis* **19**, 1198–1205.
- Harris, J. P., Edmunds, W. J., Pebody, R., Brown, D. W. & Lopman, B. A. (2008). Deaths from norovirus among the elderly, England and Wales. *Emerg Infect Dis* **14**, 1546–1552.
- Jones, M. K., Watanabe, M., Zhu, S., Graves, C. L., Keyes, L. R., Grau, K. R., Gonzalez-Hernandez, M. B., Iovine, N. M., Wobus, C. E. & other authors (2014). Enteric bacteria promote human and mouse norovirus infection of B cells. *Science* **346**, 755–759.
- Katayama, K., Murakami, K., Sharp, T. M., Guix, S., Oka, T., Takai-Todaka, R., Nakanishi, A., Crawford, S. E., Atmar, R. L. & Estes, M. K. (2014). Plasmid-based human norovirus reverse genetics system produces reporter-tagged progeny virus containing infectious genomic RNA. *Proc Natl Acad Sci U S A* **111**, E4043–4052.
- Kitamoto, N., Tanaka, T., Natori, K., Takeda, N., Nakata, S., Jiang, X. & Estes, M. K. (2002). Cross-reactivity among several recombinant calicivirus virus-like particles (VLPs) with monoclonal antibodies obtained from mice immunized orally with one type of VLP. *J Clin Microbiol* **40**, 2459–2465.
- Koo, H. L., Neill, F. H., Estes, M. K., Munoz, F. M., Cameron, A., DuPont, H. L. & Atmar, R. L. (2013). Noroviruses: the most common pediatric viral enteric pathogen at a large university hospital after introduction of rotavirus vaccination. *J Pediatric Infect Dis Soc* **2**, 57–60.
- Lay, M. K., Atmar, R. L., Guix, S., Bharadwaj, U., He, H., Neill, F. H., Sastry, K. J., Yao, Q. & Estes, M. K. (2010). Norwalk virus does not replicate in human macrophages or dendritic cells derived from the peripheral blood of susceptible humans. *Virology* **406**, 1–11.
- Papafraqkou, E., Hewitt, J., Park, G. W., Greening, G. & Vinjé, J. (2014). Challenges of culturing human norovirus in three-dimensional organoid intestinal cell culture models. *PLoS One* **8**, e63485.
- Payne, D. C., Vinjé, J., Szilagyi, P. G., Edwards, K. M., Staat, M. A., Weinberg, G. A., Hall, C. B., Chappell, J., Bernstein, D. I. & other authors (2013). Norovirus and medically attended gastroenteritis in US children. *N Engl J Med* **368**, 1121–1130.
- Ramani, S., Atmar, R. L. & Estes, M. K. (2014). Epidemiology of human noroviruses and updates on vaccine development. *Curr Opin Gastroenterol* **30**, 25–33.
- Robilotti, E., Deresinski, S. & Pinsky, B. A. (2015). Norovirus. *Clin Microbiol Rev* **28**, 134–164.
- Rockx, B., de Wit, M., Vennema, H., Vinjé, J., de Bruin, E., van Duynhoven, Y. & Koopmans, M. (2002). Natural history of human calicivirus infection: a prospective cohort study. *Clin Infect Dis* **35**, 246–253.
- Roddie, C., Paul, J. P., Benjamin, R., Gallimore, C. I., Xerry, J., Gray, J. J., Peggs, K. S., Morris, E. C., Thomson, K. J. & Ward, K. N. (2009). Allogeneic hematopoietic stem cell transplantation and norovirus gastroenteritis: a previously unrecognized cause of morbidity. *Clin Infect Dis* **49**, 1061–1068.
- Roos-Weil, D., Ambert-Balay, K., Lanternier, F., Mamzer-Bruneel, M.-F., Nochy, D., Pothier, P., Avettand-Fenoel, V., Anglicheau, D., Snanoudj, R. & other authors (2011). Impact of norovirus/sapovirus-related diarrhea in renal transplant recipients hospitalized for diarrhea. *Transplantation* **92**, 61–69.
- Saif, M. A., Bonney, D. K., Bigger, B., Forsythe, L., Williams, N., Page, J., Babiker, Z. O., Guiver, M., Turner, A. J. & other authors (2011). Chronic norovirus infection in pediatric hematopoietic stem cell transplant recipients: A cause of prolonged intestinal failure requiring intensive nutritional support. *Pediatr Transplant* **15**, 505–509.
- Schreiber, D. S., Blacklow, N. R. & Trier, J. S. (1973). The mucosal lesion of the proximal small intestine in acute infectious nonbacterial gastroenteritis. *N Engl J Med* **288**, 1318–1323.
- Schreiber, D. S., Blacklow, N. R. & Trier, J. S. (1974). The small intestinal lesion induced by Hawaii agent acute infectious nonbacterial gastroenteritis. *J Infect Dis* **129**, 705–708.
- Schwartz, S., Vergoulidou, M., Schreier, E., Loddenkemper, C., Reinwald, M., Schmidt-Hieber, M., Flegel, W. A., Thiel, E. & Schneider, T. (2011). Norovirus gastroenteritis causes severe and lethal complications after chemotherapy and hematopoietic stem cell transplantation. *Blood* **117**, 5850–5856.
- Shi, S. R., Chaiwun, B., Young, L., Cote, R. J. & Taylor, C. R. (1993). Antigen retrieval technique utilizing citrate buffer or urea solution for immunohistochemical demonstration of androgen receptor in formalin-fixed paraffin sections. *J Histochem Cytochem* **41**, 1599–1604.
- Straub, T. M., Höner zu Bentrup, K., Orosz-Coghlan, P., Dohnalkova, A., Mayer, B. K., Bartholomew, R. A., Valdez, C. O., Bruckner-Lea, C. J., Gerba, C. P. & other authors (2007). *In vitro* cell culture infectivity assay for human noroviruses. *Emerg Infect Dis* **13**, 396–403.
- Takanashi, S., Saif, L. J., Hughes, J. H., Meulia, T., Jung, K., Scheuer, K. A. & Wang, Q. (2014). Failure of propagation of human norovirus in intestinal epithelial cells with microvilli grown in three-dimensional cultures. *Arch Virol* **159**, 257–266.
- Vega, E., Barclay, L., Gregoricus, N., Williams, K., Lee, D. & Vinjé, J. (2011). Novel surveillance network for norovirus gastroenteritis outbreaks, United States. *Emerg Infect Dis* **17**, 1389–1395.
- Vongpunsawad, S., Venkataram Prasad, B. V. & Estes, M. K. (2013). Norwalk virus minor capsid protein VP2 associates within the VP1 shell domain. *J Virol* **87**, 4818–4825.
- Woodward, J. M., Gkrania-Klotsas, E., Cordero-Ng, A. Y., Aravintan, A., Bandoh, B. N., Liu, H., Davies, S., Zhang, H., Stevenson, P. & other authors (2015). The role of chronic norovirus infection in the enteropathy associated with common variable immunodeficiency. *Am J Gastroenterol* **110**, 320–327.